DSP-based integral variable structure model following control for brushless DC motor drivers

Article *in* IEEE Transactions on Power Electronics · February 1997

DOI: 10.1109/63.554169 · Source: IEEE Xplore

Tzuen-Lih Chern
National Sun Yat-sen University

Geeng-Kwei Chang
WuFeng University

DSP-Based Integral Variable Structure Model Following Control for Brushless DC Motor Drivers

Tzuen-Lih Chern, Jerome Chang, and Geeng-Kwei Chang

***Abstract*— The design and implementation of digital signal processor (DSP) microprocessor-based brushless dc motor servo control driver are presented. The integral variable structure model following control (IVSMFC) approach is presented to achieve robust accurate servo tracking. A design procedure is developed for determining the control function, the coefficients of the switching plane, and the integral control gain such that the error between the state of the model and the controlled plant is to be minimized. Simulation and experimental results show that the proposed approach can achieve accurate velocity/position servo tracking in the presence of load disturbance and plant parameter variations.**

I. Introduction

BRUSHLESS dc motors have been used widely as actuators for motion control because of their higher torque/weight ratio, maintenance freedom of commutators, lower rotor moment of inertia, and better heat dissipation. The proposed scheme for a brushless dc motor velocity/position servo control system is shown in Fig. 1. The current control loop is a sinusoidal current-controlled pulse width modulated (PWM) voltage-source inverter (VSI) which is widely applied in high-performance dc drivers. The outer control loop is designed to achieve a fast and accurate servo-tracking response under load disturbance and plant parameter variations. However, such requirements are usually difficult to achieve by using a simple linear controller. In certain cases, the variable structure control (VSC) is applied [1]–[4], but it may result in a steady-state error when there is load disturbance in it. To improve this problem, the integral variable structure control (IVSC) has been proposed in [5]. The IVSC approach comprises an integral controller for achieving a zero steady-state error under step input and a VSC for enhancing the robustness. In this paper, an integral variable structure model following control (IVSMFC) approach is presented for the outer control loop. The concept of IVSMFC methodology is to apply the (IVSC) approach to the design of a model following control system (MFCS) [6], [7]. The advantage of the IVSMFC approach is that the error trajectory, in the sliding motion, can be prescribed by the design. Also, it can achieve a rather accurate servo-tracking result and is fairly robust to plant parameter variation and external disturbances. The design of an IVSMFC system involves: 1) the choice of the control function to guarantee the existence of a sliding motion and 2) the determination of the switching function $\sigma(k)$ and the integral control gain such that the system has desired properties.

The design, simulation, and implementation of brushless dc motor servo velocity/position control systems using the IVSMFC approach is described. The implementation of the system is based on an ADSP-2105 digital signal processor (DSP) microprocessor. Simulation and experiment results are presented for demonstrating the potential of the proposed scheme.

Manuscript received April 20, 1995; revised June 7, 1996. This work was supported by National Science Council (NSC) of Taiwan, R.O.C., under project NSC85-2213-E-110-030.

The authors are with the Department of Electrical Engineering, National Sun Yat-Sen University, Kaohsiung 80424 Taiwan, R.O.C.

Publisher Item Identifier S 0885-8993(97)00421-3.

II. Synthesis of the Integral Variable Structure Model Following Controller

Let the plant be described by the following equation:

$$\dot{x}_{pi} = x_{p(i+1)} \qquad i = 1, \cdots, n-1 \tag{1a}$$

$$\dot{x}_{pn} = -\sum_{i=1}^{n} a_{pi}x_{pi} + b_pU_p - f \tag{1b}$$

where a_{pi} and b_p are the plant parameter, f are disturbances, and U_p is the control input of the plant. The reference model is represented as

$$\dot{x}_{mi} = x_{m(i+1)} \qquad i = 1, \cdots, n-1 \tag{2a}$$

$$\dot{x}_{mn} = -\sum_{i=1}^{n} a_{mi}x_{mi} + b_mU_m \tag{2b}$$

where U_m is the input command of the system.

Defining $e_i = x_{pi} - x_{mi} (i = 1, \cdots, n)$, subtracting (2) from (1), the error differential equation is

$$\dot{e}_i = e_{i+1} \qquad i = 1, \cdots, n-1 \tag{3a}$$

$$\dot{e}_n = -\sum_{i=1}^{n} a_{pi}e_i + \sum_{i=1}^{n}(a_{mi} - a_{pi})x_{mi} - b_mU_m + b_pU_p - f. \tag{3b}$$

Now one applies the IVSC approach to the error dynamics in order to synthesize the control signal U_p assuming the asymptotic convergence of the error to zero.

The IVSMFC system is shown in Fig. 2 and can be described as

$$\dot{z} = -e_1 \tag{4a}$$

$$\dot{e}_i = e_{i+1} \qquad i = 1, \cdots, n-1 \tag{4b}$$

$$\dot{e}_n = -\sum_{i=1}^{n} a_{pi}e_i + \sum_{i=1}^{n}(a_{mi} - a_{pi})x_{mi} - b_mU_m + b_pU_p - f \tag{4c}$$

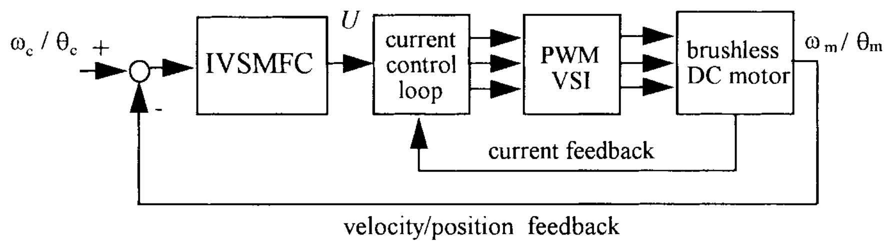

Fig. 1. Block diagram of an IVSMFC brushless dc motor velocity/position servo control system.

where the control function U_p is piecewise linear of the form

$$U_p = \begin{cases} U_p^+(e,t) & \text{if } \sigma > 0 \\ U_p^-(e,t) & \text{if } \sigma < 0 \end{cases}$$

where σ is the switching function given by

$$\sigma = c_1(e_1 - k_I z) + \sum_{i=2}^{n} c_i e_i \tag{5}$$

in which $c_i =$ constant, $c_n = 1$, and k_I is the integral control gain.

The design of such a system involves: 1) the choice of the control function U_p so that it gives rise to the existence of a sliding mode and 2) the determination of the switching function σ and the integral control gain k_I such that the system has the desired eigenvalues.

A. Choice of the Control Function

From (4) and (5), one has

$$\begin{aligned}\dot{\sigma} = {} & c_1 k_I e_1 + \sum_{i=2}^{n} c_{i-1} e_i - \sum_{i=1}^{n} a_{pi} e_i \\ & + \sum_{i=1}^{n} (a_{mi} - a_{pi}) x_{mi} - b_m U_m + b_p U_p - f. \end{aligned} \tag{6}$$

Let

$$\begin{aligned} a_{pi} &= a_{pi}^0 + \Delta a_{pi} \qquad i = 1, \cdots, n \\ b_p &= b_p^0 + \Delta b_p, \quad b_p^0 > 0, \quad \Delta b_p > -b_p^0 \end{aligned}$$

where a_{pi}^0 and b_p^0 are nominal values, and Δa_{pi} and Δb_p are the associated variations.

Let the control function U_p be decomposed into

$$U_p = U_{\text{eq}} + U_s \tag{7a}$$

where U_{eq}, called the equivalent control, is defined as the solution of the problem $\dot{\sigma} = 0$ under $f = 0, a_{pi} = a_{pi}^0, b_p = b_p^0$. That is

$$\begin{aligned} U_{\text{eq}} = \Bigg[& -c_1 k_I e_1 - \sum_{i=2}^{n} c_{i-1} e_i + \sum_{i=1}^{n} a_{pi}^0 e_i \\ & - \sum_{i=1}^{n} (a_{mi} - a_{pi}^0) x_{mi} + b_m U_m \Bigg] \Big/ b_p^0. \end{aligned} \tag{7b}$$

In the sliding motion, $\sigma = 0$, one can obtain

$$e_n = \left[-c_1(e_1 - k_I z) - \sum_{i=2}^{n-1} c_i e_i \right]. \tag{7c}$$

Substituting 7(c) into 7(b) yields

$$\begin{aligned} U_{\text{eq}} = \Bigg\{ & -c_1 k_I e_1 - \sum_{i=2}^{n-1} c_{i-1} e_i + \sum_{i=1}^{n-1} a_{pi}^0 e_i \\ & - \sum_{i=1}^{n} (a_{mi} - a_{pi}^0) x_{mi} + b_m U_m \\ & + (c_{n-1} - a_{pn}^0) \left[c_1(e_1 - k_I z) + \sum_{i=2}^{n-1} c_i e_i \right] \Bigg\} \Big/ b_p^0. \end{aligned} \tag{7d}$$

The function U_s, employed to eliminate the influence due to $\Delta a_{pi}, \Delta b_p$, and f so as to guarantee the existence of a sliding mode, is constructed as

$$U_s = \Psi_1(e_1 - k_I z) + \sum_{i=2}^{n} \Psi_i e_i + \Psi_{n+1} \tag{7e}$$

where

$$\Psi_1 = \begin{cases} \alpha_1, & \text{if } (e_1 - k_I z)\sigma > 0 \\ \beta_1, & \text{if } (e_1 - k_I z)\sigma < 0 \end{cases}$$

$$\Psi_i = \begin{cases} \alpha_i, & \text{if } e_i \sigma > 0 \\ \beta_i, & \text{if } e_i \sigma < 0 \end{cases} \qquad i = 2, \cdots, n$$

and

$$\Psi_{n+1} = \begin{cases} \alpha_{n+1}, & \text{if } \sigma > 0 \\ \beta_{n+1}, & \text{if } \sigma < 0. \end{cases}$$

It is known that the condition for the existence and reachability of a sliding motion is [8]–[10]

$$\sigma \dot{\sigma} < 0. \tag{8}$$

From (6) and (7), one can obtain

$$\begin{aligned} \dot{\sigma}\sigma = \Bigg\{ & -\sum_{i=1}^{n} \Delta a_{pi} e_i - \sum_{i=1}^{n} \Delta a_{pi} x_{mi} + (c_{n-1} - a_{pn}) e_n \\ & + (c_{n-1} - a_{pn}^0) \left[c_1(e_1 - k_I z) + \sum_{i=2}^{n-1} c_i e_i \right] \\ & + \Delta b_p U_{\text{eq}} + b_p U_s - f \Bigg\} \sigma \\ = {} & [-\Delta a_{p1} + a_{p1}^0 \Delta b_p / b_p^0 + c_1(c_{n-1} - a_{pn}^0) \\ & \cdot (1 + \Delta b_p / b_p^0) + b_p \Psi_1](e_1 - k_I z)\sigma \\ & + \sum_{i=2}^{n-1} [-\Delta a_{pi} + a_{pi}^0 \Delta b_p / b_p^0 - c_{i-1} \Delta b_p / b_p^0 \\ & + c_i (c_{n-1} - a_{pn}^0)(1 + \Delta b_p / b_p^0) + b_p \Psi_i] e_i \sigma \\ & + [-\Delta a_{pn} + (c_{n-1} - a_{pn}^0) + b_p \Psi_n] e_n \\ & + [N + b_p \Psi_{n+1}] \sigma \end{aligned} \tag{9}$$

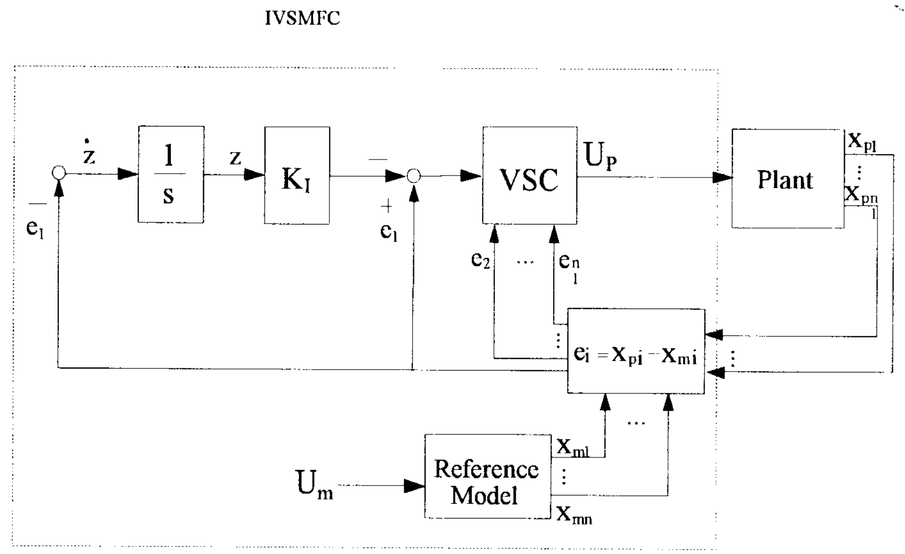

Fig. 2. The block diagram of the IVSMFC system.

where

$$
\begin{aligned}
N = &-k_I z(\Delta a_{p1} - a^0_{p1}\Delta b_p/b^0_p) \\
&- \Delta b_p/b^0_p(c_i k_I e_1) - \sum_{i=1}^{n} \Delta a_{pi} x_{mi} \\
&+ \left[-\sum_{i=1}^{n}(a_{mi} - a^0_{pi})x_{mi} + b_m U_m \right] \Delta b_p/b^0_p - f.
\end{aligned}
$$

Thus, the conditions for satisfying the inequality in (8) are shown in (10a)–(10c) at the bottom of the page.

If $\Psi_i, i = 1, \cdots, n+1$ are chosen as

$$\Psi_i = \alpha_i = -\beta_i$$

then the control function can be represented as

$$
\begin{aligned}
U_p = \Bigg\{ &-c_1 k_I e_1) - \sum_{i=2}^{n-1} c_{i-1} e_i + \sum_{i=1}^{n-1} a^0_{pi} e_i \\
&- \sum_{i=1}^{n}(a_{mi} - a^0_{pi})x_{mi} + b_m U_m \\
&+ (c_{n-1} - a^0_{pn}) \left[c_1(e_1 - k_I z) + \sum_{i=2}^{n-1} c_i e_i \right] \Bigg\} \Big/ b^0_p \\
&+ \left(\Psi_1 |e_1 - k_I z| + \sum_{i=2}^{n} \Psi_i |e_i| + \Psi_{n+1} \right) \text{sign}\,(\sigma)
\end{aligned}
\tag{11}
$$

where

$$
\begin{aligned}
\Psi_i < -\text{Sup}|[&\Delta a_{pi} - a^0_{pi}\Delta b_p/b^0 + c_{i-1}\Delta b_p/b^0_p \\
&- c_i(c_{n-1} - a^0_{pn})(1 + \Delta b_p/b^0_p)]/b_p| \\
&\text{for} \quad i = 1, \cdots, n-1 \quad \text{and} \quad c_0 = 0 \\
\Psi_n < -\text{Sup}|(&\Delta a_{pn} + a^0_{pn} - c_{n-1})/b_p|
\end{aligned}
$$

and

$$\Psi_{n+1} < -\text{Sup}|N/b_p|.$$

$$
\Psi_i = \begin{cases} a_i < \text{Inf}[\Delta a_{pi} - a^0_{pi}\Delta b_p/b^0_p + c_{i-1}\Delta b_p/b^0_p - c_i(c_{n-1} - a^0_{pn})(1 + \Delta b_p/b^0_p)]/b_p \\ \beta_i > \text{Sup}[\Delta a_{pi} - a^0_{pi}\Delta b_p/b^0_p + c_{i-1}\Delta b_p/b^0_p - c_i(c_{n-1} - a^0_{pn})(1 + \Delta b_p/b^0_p)]/b_p \end{cases}
\tag{10a}
$$

for $i = 1, \cdots, n-1$ and $c_0 = 0$

$$
\Psi_n = \begin{cases} \alpha_n < \text{Inf}[\Delta a_{pn} - c_{n-1} + a^0_{pn}]/b_p \\ \beta_n > \text{Sup}[\Delta a_{pn} - c_{n-1} + a^0_{pn}]/b_p \end{cases}
\tag{10b}
$$

and

$$
\Psi_{n+1} = \begin{cases} \alpha_{n+1} < \text{Inf}[-N]/b_p \\ \beta_{n+1} > \text{Sup}[-N]/b_p. \end{cases}
\tag{10c}
$$

B. Determination of Switching Plane and Integral Control Gain

Under ideal sliding motion, the system described by (2) can be reduced to

$$\dot{e}_i = e_{i+1} \qquad i = 1, \cdots, n-2 \tag{12a}$$

$$\dot{e}_{n-1} = -\sum_{i=1}^{n-1} c_i e_i + c_1 k_I z \tag{12b}$$

$$\dot{z} = -e_1. \tag{12c}$$

The characteristic equation of the system can be represented as

$$s^n + c_{n-1}s^{n-1} + \cdots + c_1 s + c_1 k_I = 0 \tag{13}$$

and is independent of the plant parameters; it is robust to the plant parameter variations. It is also clear that the eigenvalues can be set arbitrarily by choosing the values of $c_1, \cdots, c_{n-1}$ and k_I. Let the desired characteristic equation be

$$s^n + \alpha_1 s^{n-1} + \cdots + \alpha_n = 0.$$

Then c_i and k_I can be chosen as

$$c_{n-i} = \alpha_i \quad \text{for} \quad i = 1, \cdots, n-1$$

and

$$k_I = \alpha_n / \alpha_{n-1}.$$

III. Modeling of Brushless DC Servo Motor

The brushless dc motor considered in the paper is a three-phase permanent-magnet synchronous motor with sinusoidal back electromotive force (EMF). The voltage equation for the stator windings can be expressed as [11]

$$\begin{bmatrix} v_{as} \\ v_{bs} \\ v_{cs} \end{bmatrix} = \begin{bmatrix} R_s & 0 & 0 \\ 0 & R_s & 0 \\ 0 & 0 & R_s \end{bmatrix} \begin{bmatrix} i_{as} \\ i_{bs} \\ i_{cs} \end{bmatrix} + \frac{d}{dt} \begin{bmatrix} L_s & 0 & 0 \\ 0 & L_s & 0 \\ 0 & 0 & L_s \end{bmatrix} \begin{bmatrix} i_{as} \\ i_{bs} \\ i_{cs} \end{bmatrix} + \omega_r k_e \begin{bmatrix} \sin(\theta_r) \\ \sin(\theta_r - 2\pi/3) \\ \sin(\theta_r + 2\pi/3) \end{bmatrix} \tag{14}$$

where

- v_{as}, v_{bs}, v_{cs} the applied stator voltages;
- i_{as}, i_{bs}, i_{cs} the applied stator currents;
- R_s the resistance of each stator winding;
- L_s the inductance of the stator winding;
- ω_r the electrical rotor angular velocity;
- θ_r the electrical rotor angular displacement;
- k_e the voltage constant.

The electromagnetic torque can be expressed as

$$T_e = k_t \left[i_{as}\sin(\theta_r) + i_{bs}\sin\left(\theta_r - \frac{2\pi}{3}\right) + i_{cs}\sin\left(\theta_r + \frac{2\pi}{3}\right)\right] \tag{15a}$$

where k_t is the current constant, and P is the number of poles.

The torque, velocity, and position may be related by

$$T_e = J_m\left(\frac{2}{P}\right)\frac{d\omega_r}{dt} + B_m\left(\frac{2}{P}\right)\omega_r + T_L \tag{15b}$$

$$\theta_r = \int \omega_r \, dt \tag{15c}$$

$$\omega_m = \omega_r\left(\frac{2}{P}\right) \tag{15d}$$

where J_m is the inertia of the rotor, B_m is a damping coefficient, T_L is the load disturbance, and ω_m is the mechanical angular velocity of the rotor.

The block diagram of a brushless dc machine, portraying (14) and (15), is shown in Fig. 3.

The sinusoidal current-controlled PWM VSI as shown in Fig. 4 consists of the dc-SIN transform, current compensator, and PWM VSI circuits. The mode of the PWM VSI circuit can be simplified as a constant gain [12]

$$k_A = \frac{V_{\text{dc}}}{2E_d}$$

where V_{dc} is the dc supply voltage in the VSI, and E_d are the triangular peak values. The current loop is designed to achieve fast and accurate current tracking. In this situation, the model of the current-controlled loop can be simplified to a single-input single-output (SISO) system as shown in Fig. 5 such that the conventional methods for analyzing SISO systems may be applied with relative case.

IV. An IVSMF Controller Design for Brushless DC Motor Velocity Servo System

The dynamics of the brushless dc motor for velocity control can be described as

$$\dot{x}_{p1} = x_{p2} \tag{16a}$$

$$\dot{x}_{p2} = -a_{p1}x_{p1} - a_{p2}x_{p2} + b_p U_p - f \tag{16b}$$

where

$$a_{p1} = \frac{(R_s + g_I k_A)B_m + 3/4 P k_t k_e}{L_s J_m}$$

$$a_{p2} = \frac{R_s + g_I k_A}{L_s} + \frac{B_m}{J_m}$$

$$b_p = \frac{3/2 g_I k_A k_t}{J_m L_s}$$

$$f = \frac{R_s + g_I k_A}{J_m L_s} T_L + \frac{1}{J_m}\dot{T}_L$$

and where $x_{p1} = \omega_m$ is the mechanical angular velocity of the rotor, and U_p is the control input of the plant.

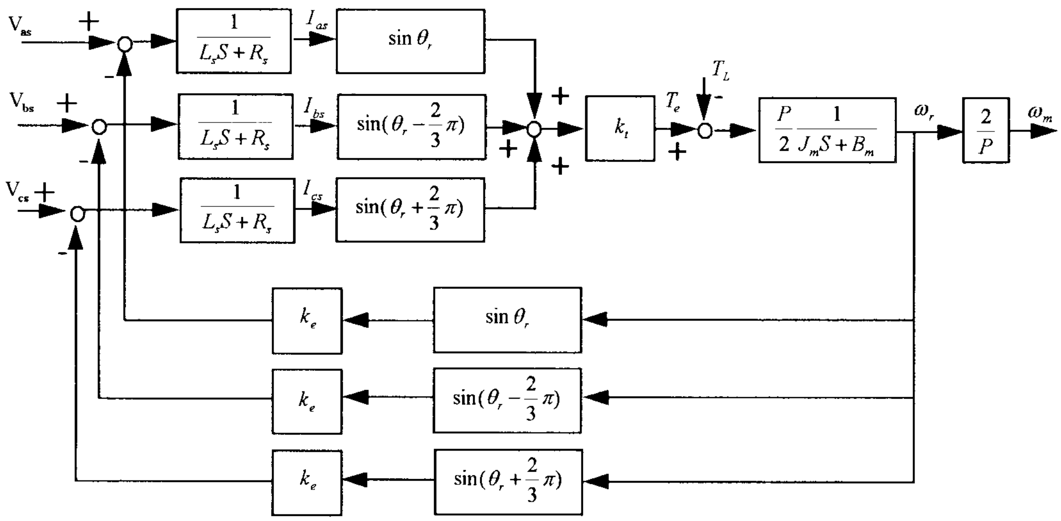

Fig. 3. Block diagram of the brushless dc motor.

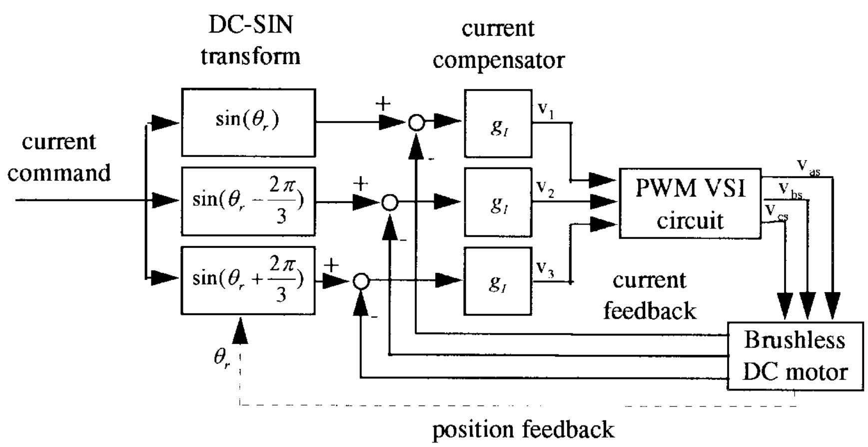

Fig. 4. Block diagram of the current-controlled PWM VSI.

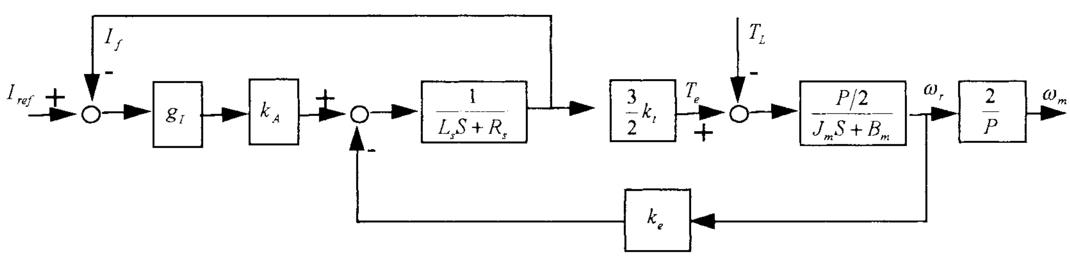

Fig. 5. The simplified dynamic model of a current-controlled loop.

The reference model is chosen as

$$\dot{x}_{m1} = x_{m2} \tag{17a}$$

$$\dot{x}_{m2} = -a_{m1}x_{m1} - a_{m2}x_{m2} + b_m U_m. \tag{17b}$$

Defining $e_i = x_{pi} - x_{mi} (i = 1, 2)$. The IVSMFC system can be represented as

$$\dot{z} = -e_1 \tag{18a}$$

$$\dot{e}_1 = e_2 \tag{18b}$$

$$\begin{aligned}\dot{e}_2 = &-a_{p1}e_1 - a_{p2}e_2 + (a_{m1} - a_{p1})x_{m1}\\ &+ (a_{m2} - a_{p2})x_{m2} - b_m U_m + b_p U_p - f.\end{aligned} \tag{18c}$$

Following the design procedure as described in Section II, one obtains

$$\begin{aligned}U_p &= U_{\text{eq}} + U_s\\ &= \left\{-c_1 k_I e_1 + a_{p1}^0 e_1 - \sum_{i=1}^{2}(a_{mi} - a_{pi}^0)x_{mi}\right.\\ &\quad \left. + b_m U_m + (c_1 - a_{p2}^0)[c_1(e_1 - k_I z)]\right\} \Big/ b_p^0\\ &\quad + (\Psi_1|e_1 - k_I z| + \Psi_2|e_2| + \Psi_3)\ \text{sign}\ (\sigma)\end{aligned} \tag{19a}$$

where

$$\Psi_1 < -\text{Sup}|[\Delta a_{p1} - a_{p1}^0 \Delta b/b^0 - c_1(c_1 - a_{p2}^0)(1 + \Delta b_p/b_p^0)]/b_p| \tag{19b}$$

$$\Psi_2 < -\text{Sup}|[\Delta a_{p2} + a_{p2}^0 - c_1]/b_p| \tag{19c}$$

and

$$\Psi_3 < -\text{Sup}|N/b_p|. \tag{19d}$$

The σ function, constructed from (5), is

$$\sigma = c_1(e_1 - k_I z) + e_2.$$

In the sliding motion, the system described by (18) can be reduced to the following simple linear form:

$$\dot{e}_1 = -c_1 e_1 + c_1 k_I z \tag{20a}$$

$$\dot{z} = -e_1. \tag{20b}$$

The characteristic equation of this reduced system is

$$s^2 + c_1 s + c_1 k_I = 0.$$

Let η_1 and η_2 be the desired eigenvalues. Then c_1 and k_I can be chosen as

$$c_1 = -(\eta_1 + \eta_2) \tag{21a}$$

$$k_I = \frac{-\eta_1 \eta_2}{\eta_1 + \eta_2}. \tag{21b}$$

V. An IVSMF Controller Design for Brushless DC Motor Position Servo System

The dynamics of the brushless dc motor for position control can be described as

$$\dot{x}_{p1} = x_{p2} \tag{22a}$$

$$\dot{x}_{p2} = x_{p3} \tag{22b}$$

$$\dot{x}_{p3} = -a_{p1}x_{p1} - a_{p2}x_{p2} - a_{p3}x_{p3} + b_p U_p - f \tag{22c}$$

where

$$\begin{aligned} a_{p1} &= 0 \\ a_{p2} &= \frac{(R_s + g_I k_A)B_m + 3/4Pk_t k_e}{L_s J_m} \\ a_{p3} &= \frac{R_s + g_I k_A}{L_s} + \frac{B_m}{J_m} \\ b_p &= \frac{3/2 g_I k_A k_t}{J_m L_s} \\ f &= \frac{R_s + g_I k_A}{J_m L_s} T_L + \frac{1}{J_m}\dot{T}_L \end{aligned}$$

and where $x_{p1} = \theta_m$ is the mechanical angular angle of the rotor, and U_p is the control input of the plant.

The reference model is chosen as

$$\dot{x}_{m1} = x_{m2} \tag{23a}$$

$$\dot{x}_{m2} = x_{m3} \tag{23b}$$

$$\dot{x}_{m3} = -a_{m1}x_{m1} - a_{m2}x_{m2} - a_{m3}x_{m3} + b_m U_m. \tag{23c}$$

Defining $e_i = x_{pi} - x_{mi} (i = 1, 2, 3)$. The IVSMFC system can be represented as

$$\dot{z} = -e_1 \tag{24a}$$

$$\dot{e}_1 = e_2 \tag{24b}$$

$$\dot{e}_2 = e_3 \tag{24c}$$

$$\dot{e}_3 = -a_{p1}e_1 - a_{p2}e_2 - a_{p3}e_3 + (a_{m1} - a_{p1})x_{m1} + (a_{m2} - a_{p2})x_{m2} + (a_{m3} - a_{p3})x_{m3} - b_m U_m + b_p U_p - f. \tag{24d}$$

Following the design procedure as described in Section II, one obtains

$$\begin{aligned} U_p &= U_{\text{eq}} + U_s \\ &= \left\{ -c_1 k_I e_1 + a_{p1}^0 e_1 + a_{p2}^0 e_2 - \sum_{i=1}^{3} (a_{mi} - a_{pi}^0) x_{mi} \right. \\ &\quad \left. + \, b_m U_m + (c_2 - a_{p3}^0)[c_1(e_1 - k_I z) + c_2 e_2] \right\} \Big/ b_p^0 \\ &\quad + (\Psi_1 |e_1 - k_I z| + \Psi_2 |e_2| + \Psi_3 |e_3| + \Psi_4) \operatorname{sign}(\sigma) \end{aligned} \tag{25a}$$

where

$$\Psi_1 < -\text{Sup}|\Delta a_{p1} - a_{p1}^0 \Delta b/b^0 - c_1(c_{n-1} - a_n^0)(1 + \Delta b/b^0)|/b_p \tag{25b}$$

$$\Psi_2 < -\text{Sup}|\Delta a_{p2} - a_{p2}^0 \Delta b/b^0 + c_1 \Delta b/b^0 - c_2(c_{n-1} - a_n^0)(1 + \Delta b/b^0)|/b_p \tag{25c}$$

$$\Psi_3 < -\text{Sup}|\Delta a_{p3} + a_{p3}^0 - c_2|/b_p \tag{25d}$$

and

$$\Psi_4 < -\text{Sup}|N/b_p|. \tag{25e}$$

The σ function, constructed from (5), is

$$\sigma = c_1(e_1 - k_I z) + c_2 e_2 + e_3.$$

In the sliding motion, the system described by (24) can be reduced to the following simple linear form:

$$\dot{e}_2 = -c_1 e_1 - c_2 e_2 + c_1 k_I z \tag{26a}$$

$$\dot{z} = -e_1. \tag{26b}$$

The characteristic equation of this reduced system is

$$s^3 + c_2 s^2 + c_1 s + c_1 k_I = 0.$$

Let λ_1, λ_2, and λ_3 be the desired eigenvalues. Then c_1, c_2, and k_I can be chosen as

$$c_1 = (\lambda_1\lambda_2 + \lambda_2\lambda_3 + \lambda_1\lambda_3) \tag{27a}$$

$$c_2 = -(\lambda_1 + \lambda_2 + \lambda_3) \tag{27b}$$

$$k_I = \frac{-\lambda_1\lambda_2\lambda_3}{\lambda_1\lambda_2 + \lambda_2\lambda_3 + \lambda_1\lambda_3}. \tag{27c}$$

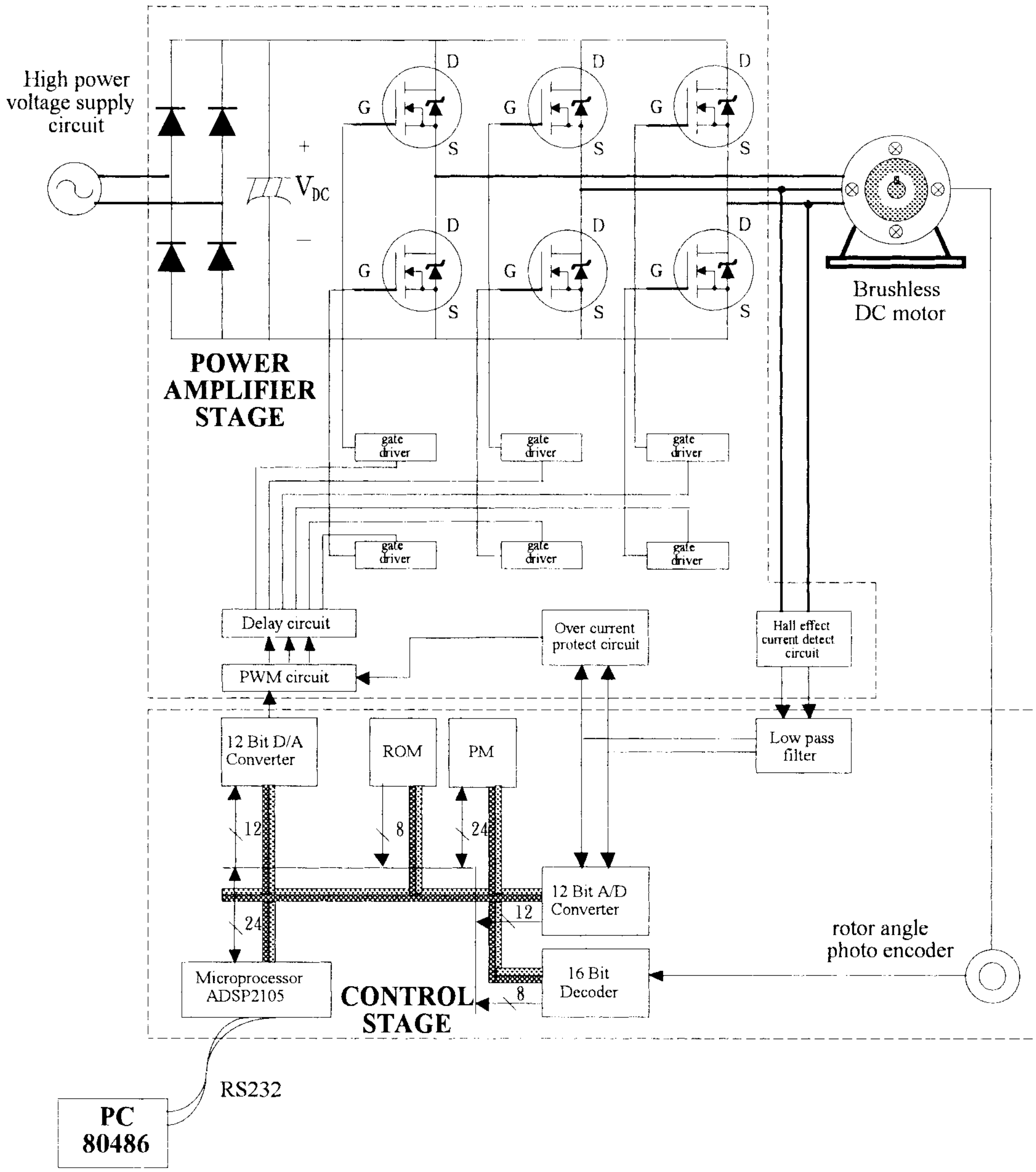

Fig. 6. The configuration of the prototype brushless dc motor driver.

VI. Experimental System Setup

To verify the performance of a proposed scheme, a prototype implementation of the brushless dc motor driver as shown in Fig. 6 consists of a power amplifier stage and control stage. The power amplifier stage includes a PWM and delay circuit, power driver circuit, power MOSFET circuit, and current detect circuit. The control stage is based on an ADSP2105 microprocessor which is a 16-b fixed point 10-MHz DSP chip. It can perform all neccessary controls such as the position, speed, acceleration and IVSMFC e.t.a. The 12-b DAC, 12-b ADC, and 16-b decoder circuits are necessary for data translation. The executive file is downloaded from the PC to the DSP through an RS-232 link. The sampling period using in this scheme is 67 μs.

VII. Simulation and Experimental Results of the Brushless DC Motor Velocity Servo Driver

The robustness of the proposed IVSMFC approach against large variations of plant parameters and external load disturbances has been simulated for demonstration. The nominal values of parameters used in this scheme are listed in Table I.

Choosing the poles of the reference model (17) at -30 and -50, one can obtain

$$a_{m1} = 1500 \quad a_{m2} = 80 \quad b_m = 1500.$$

From the poles (η_1, η_2) of the system (20) at -40 and -60, from (21), one can obtain

$$c_1 = 100 \quad k_I = 24.$$

TABLE I
SYSTEM PARAMETERS

Parameter	Value	Dimension
P	4	pole
R_s	0.79	Ω
L_s	0.00427	H
k_e	0.186	V-s/rad
k_t	0.189	N- m/A
J_m	0.00018	Kg- m^2
B_m	0.0	N-m/s
k_A	6.5	dimensionless
g_I	5.0	dimensionless

By considering operating points, one assumes the range of the plant parameter variations to be

$$|\Delta a_{p1}| < 50\% \; a_{p1}^0$$
$$|\Delta a_{p2}| < 50\% \; a_{p2}^0$$
$$|\Delta b_p| < 50\% \; b_p^0$$
$$|N| < 3000.$$

Thus, from (19), the gain Ψ_1, Ψ_2, Ψ_3 must be chosen to satisfy the following inequalities:

$$\Psi_1 < -0.0718$$
$$\Psi_2 < -0.001\,93$$
$$\Psi_3 < -0.0005.$$

And, based on simulations, one possible set of the switching gains can be chosen as

$$\Psi_1 = -0.3 \quad \Psi_2 = -0.002 \quad \Psi_3 = -0.001.$$

The simulation results of the dynamic response are plotted in Figs. 7–9. Fig. 7 shows the rotor angular velocity response and its velocity error state between the model and rotor. Figs. 8 and 9 show the velocity responses under the presence of sinusoidal load ($0.1 \sin 8\pi$t N-m) at time 0.5 s and variations of plant parameters J_m and B_m, respectively. Obviously, the IVSMFC approach is insensitive to the variation of the plant parameters and the load disturbance.

Fig. 10 shows the experimental waveforms of the brushless dc motor drive for a step change of velocity command. The dynamic characteristic indicates fast and accurate responses. Fig. 11 shows the experimental responses of angular velocity and phase current by putting a step constant load (1.5 N-m). It also shows the robustness to the load disturbance.

VIII. SIMULATION AND EXPERIMENTAL RESULTS OF THE BRUSHLESS DC MOTOR POSITION SERVO DRIVER

Choosing the poles of the reference model (23) at -15 and $-60 \pm j20$, one can obtain

$$a_{m1} = 60\,000 \quad a_{m2} = 5800 \quad a_{m3} = 135 \quad b_m = 60\,000.$$

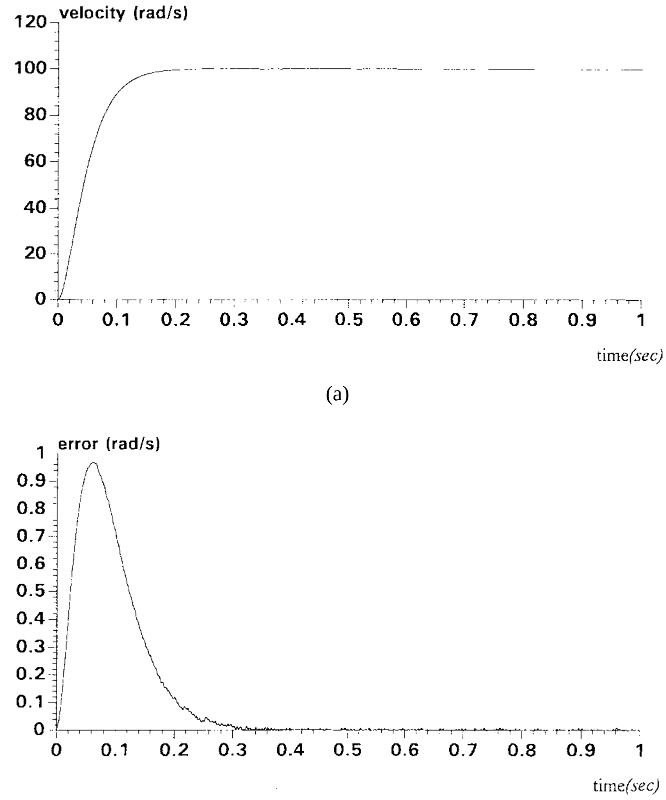

Fig. 7. Simulation responses of the brushless dc motor driver ($\omega_c = 100$ rad/s). (a) The response of the angular velocity ω_m of the rotor and (b) the velocity error state e_1 of the model and the rotor.

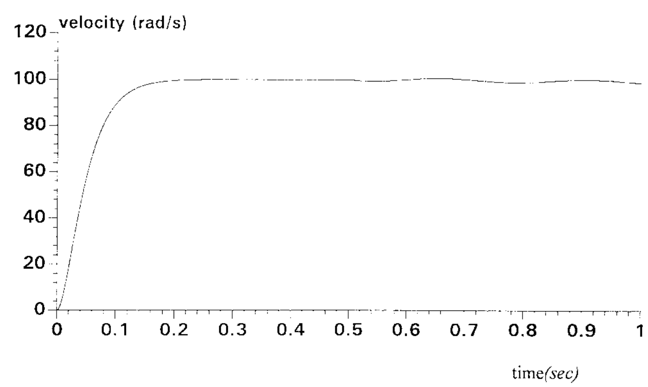

Fig. 8. Simulation responses of velocity with different kind of load placed at time 0. 5 s with sinusoidal load ($Tl = 0.1 \; \sin \; 8\pi t$ N-m; $\omega_c = 100$ rad/s).

From the poles $(\lambda_1, \lambda_2, \lambda_3)$ of the system (26) at (-60, -60, -60), from (27), one can obtain

$$c_1 = 10\,800 \quad c_2 = 180 \quad k_I = 20.$$

The gains Ψ_1, Ψ_2, Ψ_3, and Ψ_4 must be chosen to satisfy (25), and based on simulations, one possible set of the switching gains can be chosen as

$$\Psi_1 = -1 \quad \Psi_2 = -0.1 \quad \Psi_3 = -0.0005 \quad \Psi_4 = -0.001.$$

The simulation and experimental results of the dynamic response are plotted in Figs. 12–16. Fig. 12 shows the rotor angular position response and its position error state between

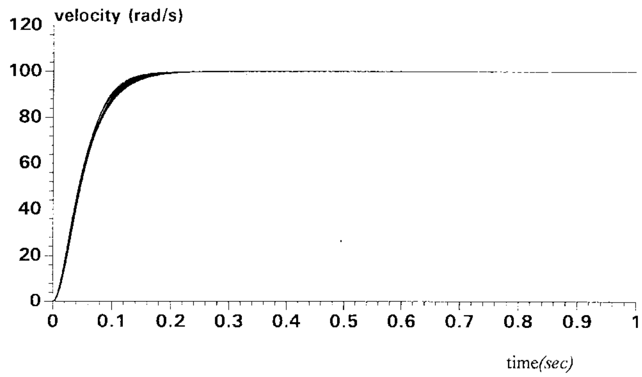

Fig. 9. Simulation of velocity response ($\omega_c = 100$ rad/s) with IVSMFC approach under random deviations of J_m from 0–300% and B_m from 0 to $+0.01$.

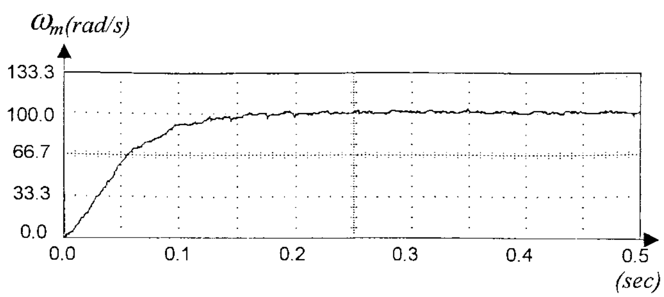

(a)

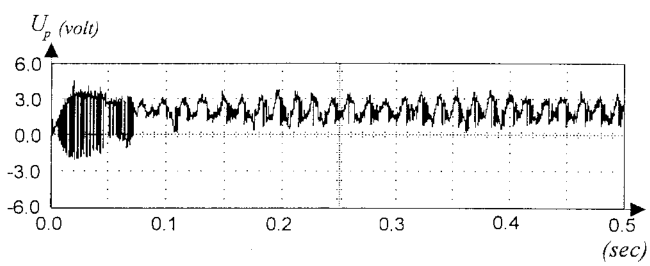

(b)

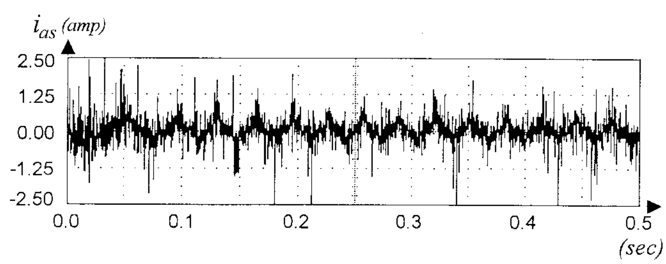

(c)

Fig. 10. Experimental result of the brushless dc motor driver ($\omega_c = 100$ rad/s). (a) The response of the angular velocity ω_m of the rotor, (b) the response of the control function U_p, and (c) the response of the phase current i_{as}.

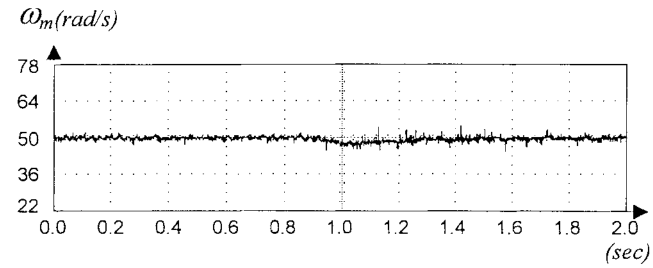

(a)

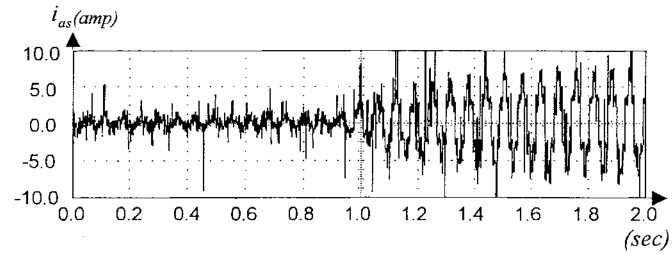

(b)

Fig. 11. Experimental results by putting a step constant load at an instant time ($Tl = 1.5$ N-m, $\omega_c = 50$ rad/s). (a) Variation of angular velocity response and (b) response of phase current i_{as}.

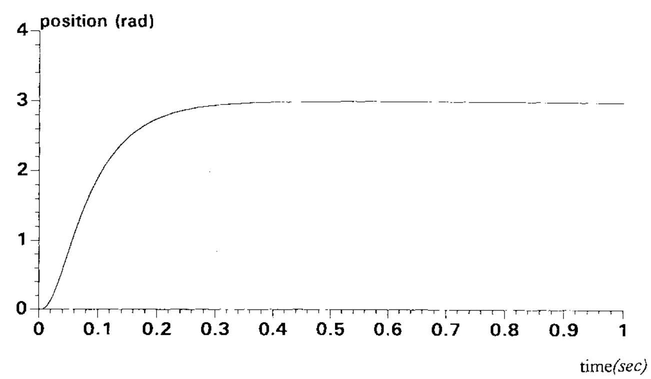

(a)

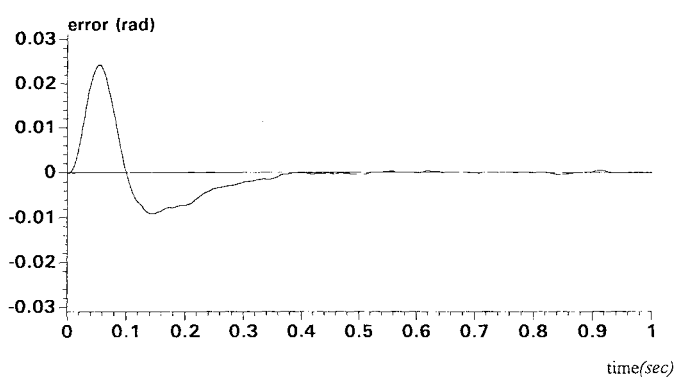

(b)

Fig. 12. Simulation responses of the brushless dc motor driver ($\theta_c = 3$ rad). (a) The response of the position θ_m of the rotor and (b) the position error state e_1 of the model and the rotor.

the model and rotor. Figs. 13–14 show the motor position control system owns robust response under a different type of load such as constant (0.4 N-m) and sinusoidal load ($0.1 sin 8\pi t$ N-m); it is robust to the variation of motor parameters J_m and B_m.

Experimental results shown in Figs. 15 and 16 behavior the fast and robust response even in both placing and removing load at an instant time. The results of the experiment also match those of simulations. From the observations, it is obvious that the proposed approach can achieve accurate and robust responses.

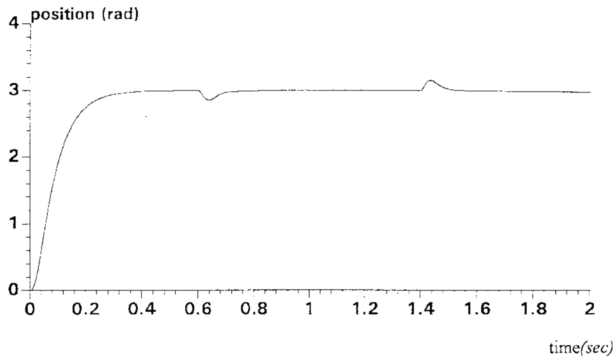

(a)

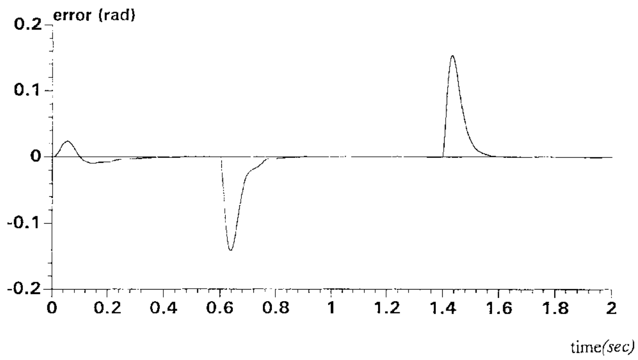

(b)

Fig. 13. Simulation results with placing and removing load (0.4 N-m) at time 0.6 and 1.4 s, respectively. (a) Position response of rotor θ_m and (b) position error response e_1.

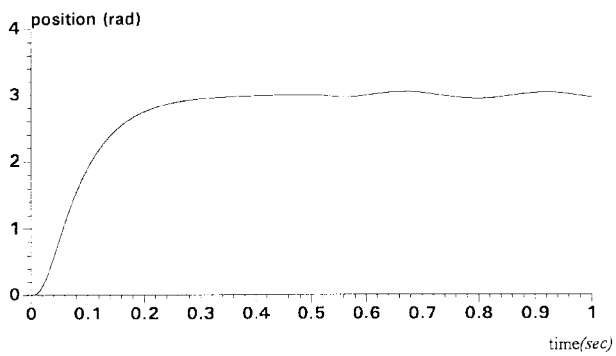

(a)

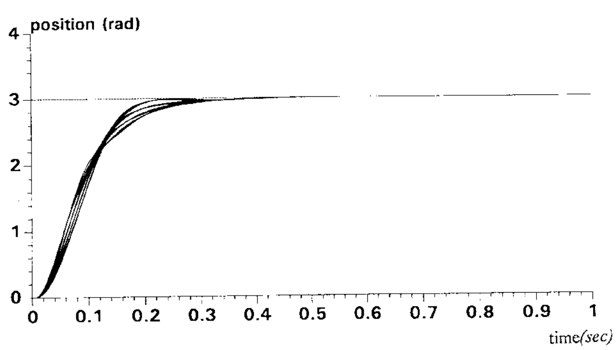

(b)

Fig. 14. Simulation of position response with sinusoidal load and random deviation in motor parameters ($\theta_c = 3$ rad). (a) The response of rotor position θ_m with sinusoidal load ($0.1 \sin 8\pi t$ N-m) at time 0.5 s. (b) The position response with an IVSMFC approach under random deviation of J_m from 0–300% and B_m from 0 to $+0.05$.

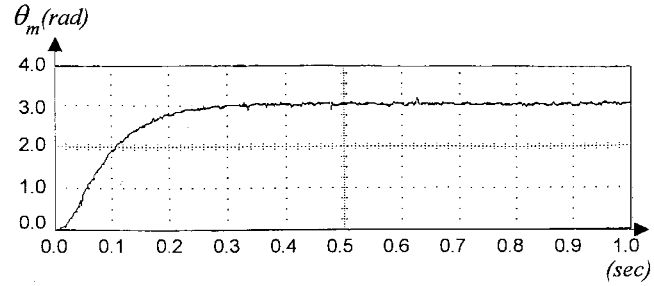

(a)

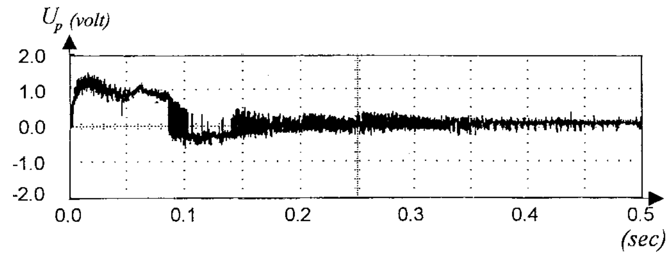

(b)

Fig. 15. Experimental result of the brushless dc motor driver ($\theta_c = 3$ rad). (a) The response of the position θ_m of the rotor and (b) the response of the control function U_p.

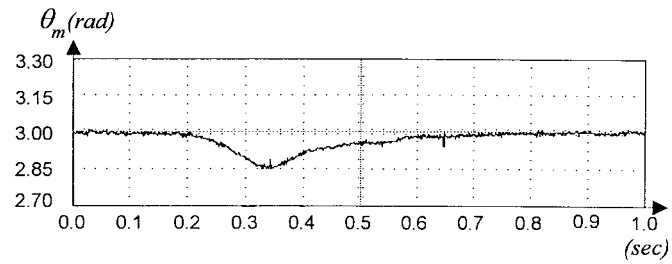

(a)

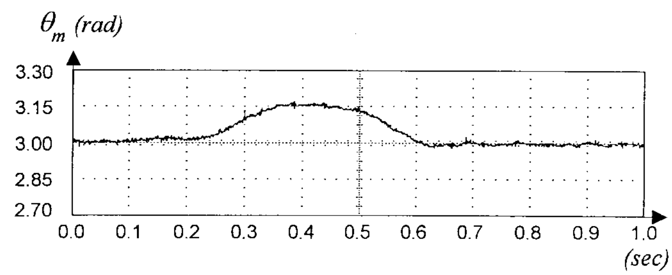

(b)

Fig. 16. Experimental results by putting and lifting load ($Tl = 0.4$ N-m). (a) The position θ_m when putting load and (b) the position θ_m when removing load at a certain instant.

IX. Conclusion

This paper presents an IVSMFC configuration and develops a procedure for determining the control function and switching plane. It has been shown that the proposed approach is theoretically robust to the plant parameter variations. A DSP-based brushless dc motor velocity/position servo control driver is presented for demonstrating the potential of the IVSMFC approach. Simulation and experimental results show that the proposed approach can achieve accurate and fast velocity/position servo tracking in the face of large parameter variations and external disturbances. It is a considerably robust and practical control law for a servomechanism system.

REFERENCES

[1] C. Rossi and A. Tonielli, "Robust control of permanent magnet motor: VSS techniques lead to simple hardware implementations," *IEEE Trans. Ind. Electron.*, vol. 41, pp. 451–460, 1994.

[2] K. W. Lim, T. S. Low, M. F. Rahman, and L. B. Wee, "A discrete time variable structure controller for a brushless dc motor drive," *IEEE Trans. Ind. Electron.*, vol. 38, pp. 102–107, 1991.

[3] J. P. Karunadasa and A. C. Renfrew, "Design and implementation of microprocessor based sliding mode controller for brushless servomotor," *Proc. Inst. Elect. Eng.*, vol. 137, pt. B., pp. 345–363, 1991.

[4] T. S. Low, K. J. Tseng, T. H. Lee, K. W. Lim, and K. S. Lock, "Strategy for the instantaneous torque control of permanent magnet brushless dc drivers," *Proc. Inst. Elect. Eng.*, vol. 138, no. 6, pt. B., pp. 355–363, 1990.

[5] T. L. Chern and Y. C. Wu, "Design of integral variable structure controller and application to electrohydraulic velocity servo systems," *Proc. Inst. Elect. Eng.*, vol. 138, pt. D., pp. 439–444, 1991.

[6] K. D. Young, "Asymptotic stability of model reference systems with variable structure control," *IEEE Trans. Automat. Contr.*, vol. AC-22, pp. 279–281, 1977.

[7] ——, "Design of variable structure model following control systems," *IEEE Trans. Automat. Contr.*, vol. AC-22, pp. 1079–1085, 1978.

[8] V. I. Utkin, "Variable structure systems with sliding modes," *IEEE Trans. Automat. Contr.*, vol. AC-22, pp. 212–222, 1977.

[9] U. Itkis, *Control Systems of Variable Structure*. New York: Wiley, 1976.

[10] V. I. Utkin, *Sliding Modes and Their Application in Variable Structure Systems*. Moscow, Russia, 1978.

[11] P. C. Krause and O. Wasynczuk, *Electromechanical Motion Devices*. New York: McGraw-Hill, 1989.

[12] D. M. Brod and D. W. Novotny, "Current control of VSI-PWM inverters," *IEEE Trans. Ind. Applicat.*, vol. IA-21, pp. 562–570, 1985.

Tzuen-Lih Chern was born in Kaohsiung, Taiwan, R.O.C., in 1958. He received the M.S. degree in 1985 and the Ph.D. degree in 1992, both from the Institute of Electronics, National Chiao Tung University, Taiwan.

From August 1987 to January 1992, he was a Lecturer at the Department of Electrical Engineering, National Sun Yat-Sen University, Taiwan. He has been an Associate Professor since February 1992. His research interests include variable structure control, ac motor drivers, and microprocessor-based control systems.

Jerome Chang was born in Kaohsiung, Taiwan, R.O.C., on January 21, 1952. He received the B.S. and M.S. degrees from the Chung Cheng Institute of Technology, Taoyuang, Taiwan, in 1975 and 1981, respectively.

He is currently working toward the Ph.D. degree from the Institute of Electrical Engineering at National Sun Yat-Sen University. His research areas are variable structure and motor drivers. He has worked in the 205th Arsenal of the Combined Services Forces of the Republic of China in instrument control, measurement control, quality control, and manufacturing process automation.

Mr. Chang is a Member of the Chinese Institute of Engineers and a Certified Engineer of Chinese Society for Quality Control.

Geeng-Kwei Chang was born in Chiayi, Taiwan, R.O.C., on June 30, 1970. He received the B.S. degree from National Cheng-Kung University, Taiwan, in 1993 and the M.S. degree from the Institute of Electrical Engineering at National Sun Yat-Sen University, in 1995.

He is currently working towards the Ph.D. degree at the Institute of Electrical Engineering. He is engaged in research of variable structure control and brushless dc motor drivers.